PERFUSION IMAGING

# Myocardial Perfusion Measurements by Spin-Labeling Under Different Vasodynamic States[#]

**Florian Fidler,[1] Christian M. Wacker,[2,*] Christian Dueren,[1] Matthias Weigel,[1] Peter M. Jakob,[1] Wolfgang R. Bauer,[2] and Axel Haase[1]**

[1]Department of Biophysics (EP5) and [2]Medical Clinic, Department of Cardiology, University of Wuerzburg, Wuerzburg, Germany

## ABSTRACT

In this study absolute myocardial perfusion was determined using a spin-labeling magnetic resonance imaging (MRI) technique at 2 Tesla. The technique was applied to 16 healthy volunteers at resting conditions, adenosine-induced stress, and oxygen breathing. Overall myocardial quantitative perfusion was determined as $2.3 \pm 0.8$ mL/g/min (rest), $4.2 \pm 1.0$ mL/g/min (adenosine), and $1.6 \pm 0.6$ mL/g/min (oxygen), respectively. $T_1$ of left ventricular blood pool decreased from $1709 \pm 101$ ms (rest) to $1423 \pm 61$ ms (oxygen), whereas $T_1$ of right ventricular blood did not change significantly ($1586 \pm 126$ ms and $1558 \pm 150$ ms). In conclusion, the presented technique for quantification of myocardial perfusion is an alternative to contrast agent-based methods. The spin labeling method is noninvasive and easily repeatable and it could therefore become an important tool to study changes in myocardial perfusion under different vasodynamic states.

*Key Words:* Magnetic resonance imaging (MRI); Spin-labeling; Coronary reserve; Perfusion quantification; Stress testing; Vasodynamics.

## INTRODUCTION

Determination of myocardial perfusion is of paramount interest in diagnosis and treatment of coronary artery disease (CAD), since alterations of perfusion are more closely related to the functional significance of a coronary artery stenosis than to the morphology of the stenosis itself (Gould and Lipscomb, 1974; Sawada et al., 1995; Shelton et al., 1993; Wilson et al., 1987).

Most MRI approaches that determine perfusion are based on first-pass techniques, i.e., one observes signal dynamics after application of a contrast agent (Manning et al., 1991; Schaefer et al., 1979; Wilke et al., 1993, 1994, 1995, 1997). The signal dynamics are related to concentration dynamics, and perfusion is obtained either qualitatively by empirical parameters or quantitatively by deconvolution of the concentration time curve (Jerosch-Herold et al., 1998). However, despite its widespread use in myocardial perfusion imaging, the disadvantages of first-pass techniques are well known, e.g., measurements are not easily repeatable and data have to be unfolded with an arterial input function.

Spin-labeling techniques exploit the labeling of the nuclear magnetization of water protons either by direct preparation of inflowing (arterial) spins or by specific preparation of the imaging slice and leaving the inflowing spins in thermo-magnetic equilibrium. In both cases water is used as a free, diffusible, contrast agent. This endogenous, contrast agent technique is easily repeatable, but at the expense of a low contrast to noise ratio (CNR). Direct, arterial spin-labeling techniques for myocardial perfusion measurements were done in isolated rat hearts in the early 1990s (Williams et al., 1993); however, the complex geometry of the heart and the supplying vessels hampered the application of this technique for the in vivo heart. Bauer et al (1997) proposed slice-selective inversion in the isolated, cardioplegic rat heart with the advantage of applying this method to the in situ heart. It was demonstrated that variations in the myocardial perfusion directly reflect changes of the apparent $T_1$ relaxation time (Bauer et al., 1997). To separate inflow-related and stationary relaxation effects, $T_1$ measurements after slice-selective and global-spin preparation were performed, and this approach was applied to rat myocardium in vivo (Belle et al., 1998; Kahler et al., 1997) and human hearts (Bock et al., 1997; Poncelet et al., 1999; Wacker et al., 1999, 2002).

The application to the human heart is limited due to myocardial and breathing motion. Since breathing motion can be controlled by breathhold or gating techniques (Poncelet et al., 1999), myocardial motion needs an exact sequence timing and proper cardiac triggering to minimize error due to misalignment of spin preparation and imaging slice. Electrocardiogram (ECG) triggering has been reported to be the major problem in Wacker et al. (1999, 2002).

The objective of this study was a quantitative analysis of myocardial perfusion assessed by spin-labeling at rest and after vasodilation and demonstration of the coronary autoregulation in the human heart at 2 Tesla.

## MATERIALS AND METHODS

### Quantitative Perfusion Evaluation

Spin-labeling used in this work is based on $T_1$ measurements after global and slice-selective spin preparation. Due to the inflow of unsaturated proton spins, $T_1$ in tissue is shortened after the slice-selective, preparation case compared to global saturation. Bauer et al. (1997) showed that, assuming a two compartment model with fast proton exchange between the compartments, the absolute perfusion P in (mL/g/min) can be calculated as

$$ P = \frac{\lambda}{T_{1blood}} \left( \frac{T_{1global}}{T_{1selective}} - 1 \right) \qquad (1) $$

where the blood tissue partition coefficient $\lambda$ represents the quotient of water content of capillary blood and perfused tissue, which in myocardial tissue is $\sim 0.9$ (mL/g) (Reeder et al., 1996). $T_{1blood}$ is the longitudinal relaxation time of the arterial blood, measured in the left ventricle (LV). $T_{1global}$ and $T_{1selective}$ is the myocardial $T_1$ calculated after the respective spin preparation. Perfusion reserve is calculated as the quotient of perfusion under adenosine-induced stress and perfusion at rest.
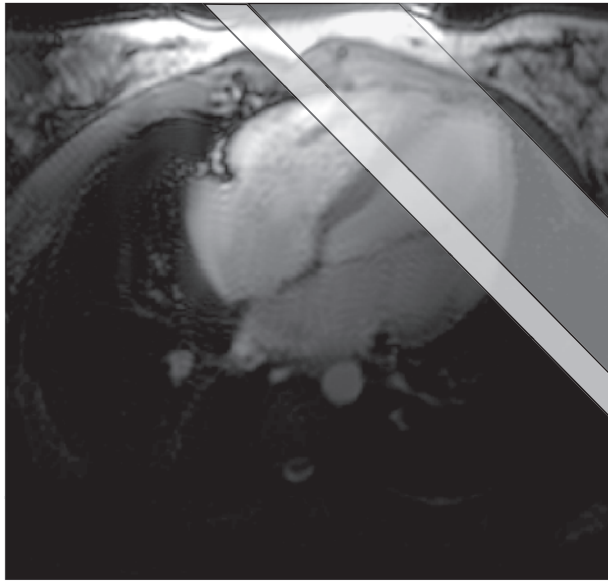
### $T_1$ Measurements

Pulse sequences were implemented on a 2 Tesla whole body scanner (Bruker, Ettlingen, Germany) with a maximal gradient strength of 31 mT/m and a rise time of 600 μsec. This system was equipped with an External Signal Synchronization (ESS) trigger system (Bruker) with an optical connected ECG sensor. The signal was received with a homemade quadrature surface coil with two, noise-matched preamplifiers directly attached to the coil for each quadrature channel to optimize signal-to-noise ratio (SNR) for the single-receiver MR system (Fidler et al., 2000). Adjustments and setup was done with ECG-gated scout FLASH images.

For determination of $T_1$, we implemented a fast, ECG-gated, saturation recovery FLASH sequence (Bock et al., 1997; Haase et al., 1986; Wacker et al., 1999). Between a 40 ms spin preparation consisting of five 90° pulses followed by spoiler gradients and a FLASH readout a progressing recovery delay $T_S$ leads to set of images, which allows quantification of appropriate $T_1$.

One image for equilibrium magnetization and nine images with progressing recovery delays $T_S$ (100, 200, 300, 400, 600, 800, 1000, 1200, and 1400 ms) were

*Figure 1.* Long-axis scout showing position of double oblique, short-axis measurement slice (light gray). Dark gray bar shows the saturation slab for slice-selective measurements. Overlap of saturation slab was 2 mm.

obtained. For each $T_S$ an initial ECG-trigger delay was adjusted automatically by heart rate to acquire end-diastolic images. The readout module was a centric reordered FLASH image with phase rewinder ($T_R/T_E/\alpha$/FOV/SL/Matrix/SW = 2.9 ms/1.4 ms/5°/300 mm/12 mm/128 × 80/780 Hz per pixel). Acquisition time per image was 230 ms. Spin preparation was done globally and was slice selective. The global preparation saturated the whole probe, while slice-selective preparation labeled the readout slice down to the apex of the heart with a 60 mm saturation slab (Fig. 1). This slab was placed automatically with an overlap of the imaging slice of 2 mm (Reeder et al., 1996). The $T_1$ technique was validated in a calibrated, stationary $T_1$ phantom and showed no systematic deviations to the measured $T_1$ values for global and selective presaturation. Each dataset consisting of 10 images was obtained in a single breathhold period of 14 sec to 18 sec, depending on individual heart rate.

## Volunteers and Measurement Protocol

Informed consent was obtained prior to the study, which was approved by the local ethics committee. Sixteen healthy volunteers (13 male/3 female, aged 27±9 years) were examined after being informed about the protocol and possible side effects of adenosine. Heart rate was continuously monitored and blood pressure was monitored before and during adenosine-induced vasodilation. The commands for breath holding were practised with the subject outside the scanner to improve breathhold capabilities and reduce diaphragm shift during breathhold, thus improving image quality.

A 5-minute adjustment and positioning of the double oblique, mid-ventricular, short-axis view was done for experimental setup. In all volunteers, five to 10 $T_1$ measurements after global and slice-selective spin preparation, respectively, were performed at rest (Figs. 2 and 3). In 10 volunteers measurements were performed at rest and while applying adenosine with a dose of 0.14 mg/kg/min via an antecubital vein. In seven volunteers exams were done under oxygen breathing within 15 to 20 minutes and while the subject inhaled room air. One volunteer underwent both adenosine and oxygen protocol within one exam. Total examination time for each volunteer was about 45 min in a preselected, single slice.

Oxygen was applied by a mask system (Positive End-expiratory Pressure System, Peep) with a flow of 12 L/min, which extends normal breathing volume. This mask system consists of a close-fitting mouthpiece connected by a one-way valve to the oxygen supply with a 2-liter puffer bag and another one for disposal of exhaled air to the scanner room.
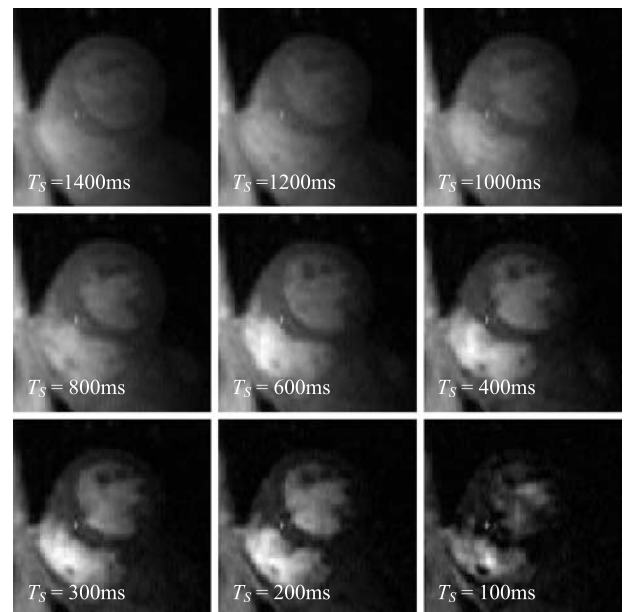


*Figure 2.* Amplitude images of a healthy volunteer with slice-selective spin preparation obtained in a single breathhold (room air). The corresponding saturation recovery delays $T_S$ are displayed in each image.
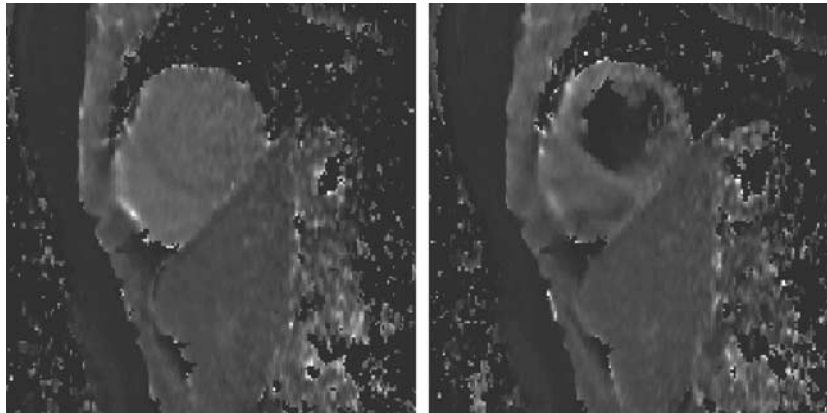
**Figure 3.** Representative $T_1$ map after global spin preparation (left) and slice-selective saturation (right), each obtained in a single breathhold period (rest, room air). Fit of $T_1$ is performed pixel-based with a three-parameter, exponential fit.

## Data Evaluation

Acquired images were evaluated on an offline Linux workstation using an individually written software package for image segmentation. Regions of interest (ROI) were the entire myocardium of LV and the blood pool of LV and right ventricle (RV). To minimize partial volume effects of blood pool, the ventricular wall was not included in segmentation. As a quality control of the measurements, body fat and skeletal muscle were also inspected. Segmentation was performed manually in each image. Image series showing breathing artifacts in a fast cine loop were rejected.

$T_1$ from measured image intensity in the ROI was fitted with a three-parameter, exponential fit using commercial statistics software (Origin, Microcal, Northampton, MA).

The statistical significance p of changes in $T_1$ under resting conditions, adenosine, and oxygen breathing was calculated by Student's t-test. Values are given as mean $T_1$ values ± standard deviation (SD).

Acquired images could be displayed in a fast cine loop, and in critical cases upon request a $T_1$ map (pixel by pixel) could be calculated immediately after image acquisition to appraise the quality of images and breathhold. Calculation time for a pixel-based map was about 1 minute (Silicon Graphics, O2 300 Mhz).
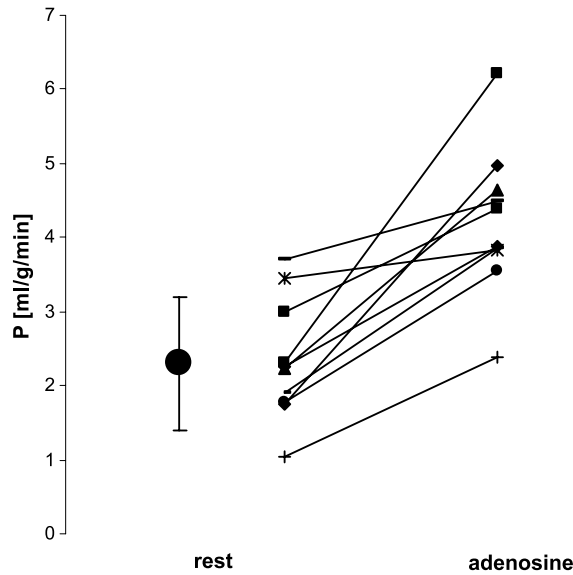
## RESULTS

The results of the $T_1$ measurements after global and slice-selective spin preparation assessed in different tissues at three different conditions (room air, adenosine-induced vasodilation, and oxygen breathing) are summarized in Table 1. All examined subjects were evaluated. A total of 18 breathholds were rejected from data evaluation (five due to ECG failure, four to insufficient breathholding, and nine due to scanner errors); these measurements were repeated.

Using Eq. 1, quantitative perfusion P was calculated as 2.3±0.8 mL/g/min (rest), 4.2±1.0 mL/g/min (adenosine, Fig. 4), and 1.6±0.6 mL/g/min (oxygen, Fig. 5), respectively. $T_1$ of skeletal muscle and fat did not change significantly ($0.12 < p < 0.47$). The results of one volunteer undergoing both adenosine stress and oxygen breathing within one exam are shown in Fig. 6.

**Table 1.** Values for $T_1$ in (ms) after slice-selective and global (given in brackets) preparation and perfusion P (mL/g/min).

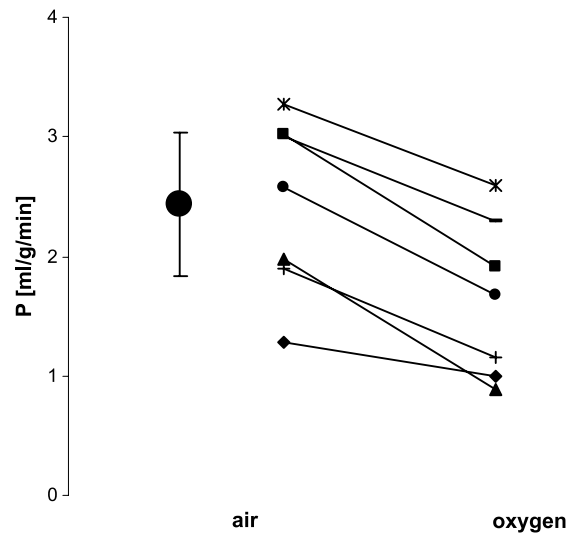| | P (ml/g/min) | $T_1$(myo) (ms) | $T_1$(LV) (ms) | $T_1$(RV) (ms) | $T_1$(sm) (ms) | $T_1$(fat) (ms) |
|---|---|---|---|---|---|---|
| *Room air* | 2.3±0.8 | 1183±56 (1265±49) | (1709±101) | (1586±126) | 1030±55 (1032±54) | 294±15 (292±14) |
| *Adenosine* | 4.2±1.0 | 1124±50 | – | – | 1033±79 | 291±29 |
| *O₂* | 1.6±0.6 | 1291±75 (1389±60) | (1423±61) | (1558±150) | 1028±63 (1036±53) | 289±17 (290±14) |

Values are given as mean ± SD. $T_1$ is given for myocardium (myo), left and right ventricular blood pool (LV, RV), skeletal muscle (sm), and fat.
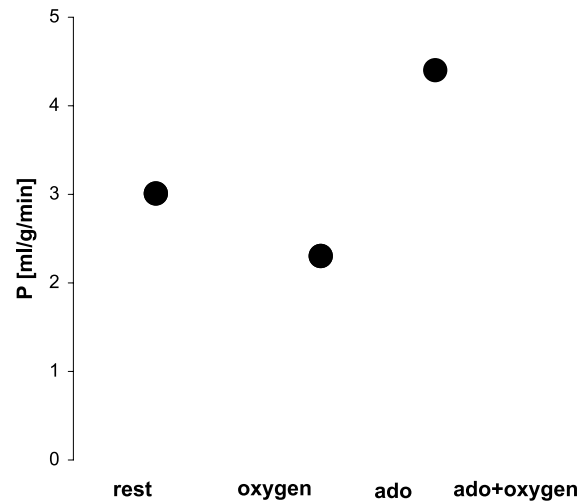
**Figure 4.** Myocardial perfusion P under room air and adenosine-induced vasodilation (n=10) (p<0.0005); error bars: SD.



**Figure 6.** Changes in myocardial perfusion P under room air and oxygen breathing, adenosine (ado) and adenosine plus oxygen breathing assessed within one exam in one volunteer.

### DISCUSSION

In this pilot study we could show that absolute quantification of myocardial perfusion is possible using the presented spin-labeling MRI technique at 2 Tesla. Myocardial perfusion was assessed under different vasodynamic states of the coronary system, i.e., resting, adenosine-induced hyperperfusion, and oxygen breathing.

Perfusion was averaged over the entire myocardium contained in a single slice. Vasodilation was induced by adenosine, and a demonstration of coronary autoregulation was performed by application of oxygen. The latter is based on the fact that coronary autoregulation decreases coronary flow under hyperbaric oxygen conditions to balance oxygen consumption and oxygen supply (Ribeiro et al., 1979; Rivas et al., 1980). As predicted by theory (Bauer et al., 1997), changes in the apparent $T_1$ measured following global-spin preparation were different from those measured following slice-selective, spin preparation. A further significant adenosine-induced change in $T_1$ should only occur with slice-selective preparation due to the inflow of nonsaturated spins. This hypothesis was substantiated by our study, showing a decrease in myocardial $T_1$, whereas $T_1$ of skeletal muscle did not change after adenosine (Wacker et al., 1999).

Obtained values for perfusion at rest and after vasodilation are constantly lower than values reported recently using a similar imaging technique (Wacker et al., 1999). In this former study, overestimation of $T_1$ values and consecutive myocardial perfusion were due

Myocardial $T_1$ remains almost constant under extended oxygen consumption in the limits of 1389±60 ms (rest) and 1351±65 ms (oxygen).

$T_1$ of left ventricular blood pool decreased from 1709±101 ms (rest) to 1423±61 ms (oxygen) (p<0.0005), whereas $T_1$ of right ventricular blood did not change significantly (1586±126 ms and 1558±150 ms, p=0.7).



**Figure 5.** Myocardial perfusion P under room air and oxygen breathing (n=7) (p<0.1); error bars: SD.

to the lack of exact ECG triggering due to hardware limitations. This hindrance implied that due to the low spatial resolution involved in this method, an inherent, broadened, point spread function resulted in a significant contamination of the myocardial signal with that of the left ventricle. Hence, high blood flow in the ventricle could result in overestimation of perfusion. However, in our study this problem could be overcome with ECG triggering ''on-the-fly'': exact timing within ECG cycle and automatic calculation of appropriate trigger delays for different saturation times led to data acquisition at exactly the same time during diastole for all images. As a consequence, obtained values for absolute perfusion and perfusion reserve are more precise. Perfusion reserves correlate well with values from literature, whereas quantitative perfusion is overestimated by a factor of approximately two (Gould and Lipscomb, 1974; Hutchins et al., 1990; Jerosch-Herold et al., 1998; Lida et al., 2000; Manning et al., 1991; Sawada et al., 1995; Schaefer et al., 1979; Shelton et al., 1993; Wilke et al., 1994, 1995, 1997; Wilson et al., 1987). A possible reason for the calculated, higher perfusion values could be an overestimation of the true, adenosine-induced difference in $T_1$ owing to measurement inaccuracy. The calculation of absolute perfusion P is not only influenced by the parameter $T_{1selective}$, but also by $T_{1global}$ and $T_{1blood}$, which have to be determined by different measurements. Therefore, inaccuracies in $T_{1selective}$, $T_{1global}$, and $T_{1blood}$ estimations could lead to the difference in perfusion values P (Wacker et al., 1999).

During hyperoxygenation, the effect of physically dissolved paramagnetic oxygen on reduction of $T_1$ was observed in left ventricular blood (Hueckel et al., 2000). A significant reduction in myocardial perfusion of about 35% was observed, which is in agreement with results recently reported (Fidler et al., 2000; Ribeiro et al., 1979). The basic principle of this phenomenon is that the coronary vascular system tries to balance oxygen supply and demand, a mechanism that is referred to as coronary autoregulation. Future studies in patients have to show if determination of autoregulation is possible and provides diagnostic information e.g., in patients with coronary artery disease or hypertensive heart diseases.

A perfect match of saturation slab to imaging slice is limited, since the slice profiles of the excitation pulse and saturation slab still differ to a certain extent. This could be optimized in a stationary phantom showing no significant perfusion, and an extra gap of 2 mm should lock out overestimation of perfusion due to slight heart movement in diastole and between different cardiac cycles, but nevertheless, this introduces an additional, unwanted source of error.

Sequence timing was optimized to assure spin preparation and readout in the same cardiac phase. Changes or arrhythmias in cardiac cycle or diaphragm shift during evolution delay $T_S$ of the preparation were not monitored, i.e., by navigator techniques and may lead, especially in patient studies, to an error based on cardiac function. Cardiac movement between preparation and readout is not problematic, since labeled spins are moved back to their original positions in the cardiac cycle.

For perfusion evaluation, vascular geometry and blood flow of arterial macrovessels are ignored, which is suspected to be a source for overestimation of perfusion (Ye et al., 1997). The venous contribution can be minimized by spatial presaturation as described in (Reeder et al., 1996). The tissue model used for perfusion evaluation relies on the assumption that capillaries in myocardium are mainly oriented parallel in a long-axis direction. Based on (Kassab and Fung, 1994) this assumption is good for mid- and epimyocardium, but in endo-myocardium (where capillaries are orientated oblique) this may lead to an underestimation of perfusion. However, in this study, only the averaged information of ventricular wall was used, and the main orientation of ascending and descending vessels was parallel to the long axis.

Major problems in data acquisition due to irregularities caused by breathholds or arrhythmias are quickly detected online by the suggested cine-loop and/or pixel-based $T_1$ maps, and measurements can immediately be repeated if necessary.

Diaphragm shift during breathhold was minimized by a previous training outside the magnet, but still some breathholds were rejected from evaluation. Monitoring of breathhold quality and slice alignment between repetitive breathhold periods can be done with the acquired images, since the diaphragm is included in the resulting images.

Although the surface coil used in the present study was optimized for the single receiver chain of the scanner, contrast to noise could be improved using a dedicated cardiac array coil. Due to the low CNR obtained from the experimental data in this study, only averaged, overall, myocardial perfusion is calculated. A further optimized readout module such as the segmented echo planar (EPI) readout might allow segmentation of myocardial segments. Estimating regional perfusion as in contrast, agent-based methods was limited by the contrast-to-noise ratio and has to be shown in future studies, e.g., at 3 T scanners. The presented method benefits from increased signal-to-noise ratio of high field strength and increased label appearance due to longer $T_1$. Furthermore, future developments must

extend this technique from a single-slice to a multi-slice technique to scan several slices. Such an extension would allow a scan of the entire heart in a reasonably short time.

## CONCLUSION

The presented spin-labeling technique provides an easy and robust tool for noninvasive assessment of myocardial perfusion and perfusion reserve. Even if absolute perfusion is overestimated due to inaccuracies in $T_1$ estimation, obtained values for perfusion reserve are close to known values. Using oxygen as an intrinsic contrast agent might overcome limitations of approaches using extrinsic contrast agents. Studies in patients with coronary artery disease are now warranted comparing the presented $T_1$ technique with first-pass MRI and myocardial scintigraphy to show the clinical impact of this new method.

## ACKNOWLEDGMENT

## REFERENCES

Bauer, W. R., Roder, F., Hiller, K. H., Han, H., Fröhlich, S., Rommel, E., Haase, A., Ertl, G. (1997). The effect of perfusion on $T_1$ after slice selective spin inversion in the isolated cardiophlegique rat heart. *Magn. Reson. Med.* 38:917–923.

Belle, V., Kahler, E., Waller, C., Rommel, E., Voll, S., Hiller, K. H., Bauer, W. R., Haase, A. (1998). In vivo quantitative mapping of cardiac perfusion in rats using a noninvasive MR spin-labeling method. *J. Magn. Reson. Imaging* 8:1240–1245.

Bock, M., Bauer, W. R., Hillenbrand, H., Schad, L. R. (1997). $T_1$-Maps of the Human Heart Acquired in a Single Breathhold. Vancouver: Proc. ISMRM.

Fidler, F., Förster, A., Griswold, M., Nittka, M., Haase, A. (2000). Noise Matched ''Solder & Go'' Modular Low Noise Preamplifier for Surface Coils. Paris: Proc. ESMRB.

Gould, K. L., Lipscomb, K. (1974). Effects of coronary stenosis on coronary flow reserve and resistance. *Am. J. Cardiol.* 34:48–55.

Haase, A., Frahm, J., Matthaei, D., Hänicke, W., Merboldt, D. (1986). FLASH imaging: rapid NMR imaging using low flip angle pulses. *J. Magn. Reson.* 67:258–266.

Hueckel, P., Schreiber, W. G., Markstaller, K., Bellemann, M., Kauczor, H. U., Thelen, M. (2000). Effect of Partial Oxygen Pressure and Hematocrit On $T_1$ Relaxation in Human Blood. Denver: Proc. ISMRM.

Hutchins, G. D., Schwaiger, M., Rosenspire, K. C., Krivokapich, J., Schelbert, H., Kuhl, D. E. (1990). Noninvasive quantification of regional blood flow in human heart using N-13 ammonia and dynamic positron emission tomographic imaging. *J. Am. Coll. Cardiol.* 15(5):1032–1042.

Jerosch-Herold, M., Wilke, N., Stillman, A. E., Wilson, R. F. (1998). Magnetic resonance quantification of myocardial perfusion reserve with a Fermi function model for constrained deconvolution. *Med. Phys.* 25(1):73–84.

Kahler, E., Belle, V., Waller, C., Rommel, E., Hiller, K. H., Voll, S., Bauer, W. R., Haase, A. (1997). Quantitative Determination of Perfusion and Regional Blood Volume in Rat Myocardium In Vivo. Brusel: Proc. ESMRMB.

Kassab, G. S., Fung, Y. C. (1994). Topology and dimensions of pig coronary capillary network. *Am. J. Physiol.* 267:H319–H325.

Lida, H., Yokohama, I., Agostini, D., Banno, T., Kato, T., Ito, K., Kuwabara, Y., Oda, Y., Otake, T., Tamura, Y., Tadamura, E., Yoshida, T., Tamaki, N. (2000). Quantitative assessment of regional myocardial blood flow using oxygen-15-labelled water and positron emission tomography: a multi-centre evaluation in Japan. *Eur. J. Nucl. Med.* 27(2):192–201.

Manning, W. J., Atkinson, D. J., Grossman, W., Paulin, S., Edelman, R. R. (1991). First-Pass nuclear magnetic resonance imaging studies using gadolinium-DTPA in patients with coronary artery disease. *J. Am. Coll. Cardiol.* 18:959–965.

Poncelet, B. P., Koelling, T. M., Schmidt, C. J., Kwong, K. K., Reese, T. G., Ledden, P., Kantor, H. L., Brady, T. J., Weisskoff, R. M. (1999). Measurement of human myocardial perfusion by double-gated flow alternating inversion recovery EPI. *Magn. Reson. Med.* 41:510–519.

Reeder, S. B., Atalay, M. K., McVeigh, E. R., Zerhouni, E. A., Forder, J. R. (1996). Quantitative cardiac perfusion: a noninvasive spin-labeling method that exploits coronary vessel geometry. *Radiology* 200(1):177–184.

Ribeiro, L. G., Louie, E. K., Davis, M. A., Maroko, P. R. (1979). Augmentation of collateral blood flow to the ischaemic myocardium by oxygen inhalation

following coronary artery occlusion. *Cardiovasc. Res.* 13(3):160–166.

Rivas, F., Rembert, J. C., Bache, R. J., Cobb, F. R., Greenfield, J. C. Jr. (1980). Effect of hyperoxia on regional blood flow after coronary occlusion in awake dogs. *Am. J. Physiol.* 238(2):H244–H248.

Sawada, S., Muzik, O., Beanlands, R. S. B., Wolfe, E., Hutchins, G. D., Schwaiger, M. (1995). Interobserver and interstudy variability of myocardial blood flow and flow reserve measurements with nitrogen 13 ammonialabeled positron emission tomography. *J. Nucl.* 2:413–422.

Schaefer, W., Wuesten, B., Schaper, W., eds. (1979). The Pathophysiology of Myocardial Perfusion Amsterdam: Elsevier/North-Holland Biomedical Press, 415–470.

Shelton, M. E., Sennef, M. J., Ludbrook, P. A., Sobel, B. E., Bergmann, S. R. (1993). Concordance of nutritive myocardial perfusion reserve and flow velocity reserve in conductance vessel in patients with chest pain with angiographical normal coronary arteries. *J. Nucl. Med.* 34:717–722.

Wacker, C. M., Bock, M., Hartlep, A. W., Beck, G., Kaick, G. V., Ertl, G., Bauer, W. R., Schad, L. R. (1999). Changes in myocardial oxygenation and perfusion under pharmacological stress with dipyridamol: assessment using $T_2^*$ and $T_1$ measurements. *Magn. Reson. Med.* 41:686–695.

Wacker, C. M., Wiesmann, F., Bock, M., Jakob, P. M., Sandstede, J. J. W., Lehning, A., Ertl, G., Schad, L. R., Haase, A., Bauer, W. R. (2002). Determination of regional blood volume and intra- extra-capillary water exchange in human myocardium using feruglose: first clinical results in patients with coronary artery disease. *Magn. Reson. Med.* 47:1013–1016.

Wilke, N., Simm, C., Zhang, J., Ellermann, J., Ya, X., Merkle, H., Path, G., Ludemann, H., Bache, R. J.,

Ugurbil, K. (1993). Contrast-enhanced first pass myocardial perfusion imaging: correlation between myocardial blood flow in dogs at rest and during hyperemia. *Magn. Reson. Med.* 29:485–497.

Wilke, N., Jerosch-Herold, M., Stillman, A. E., Kroll, K., Tsekos, N., Merkle, H., Parish, T., Hu, X., Wang, Y., Bassingthwaighte, J., Bache, R. J., Ugurbil, K. (1994). Concepts of myocardial perfusion imaging in magnetic resonance imaging. *Magn. Reson. Q* 10:249–286.

Wilke, N., Kroll, K., Merkle, H., Wang, Y., Ishibashi, Y., Xu, Y., Zhang, J., Jerosch-Herold, M., Muhler, A., Stillman, A. E., Ugurbil, K. (1995). Regional myocardial blood volume and flow: first-pass MR imaging with polylysine-Gd-DTPA. *J. Magn. Reson. Imaging* 5:227–237.

Wilke, N., Jerosch-Herold, M., Wang, Y., Huang, Y., Christensen, B. V., Stillman, A. E., Ugurbil, K., McDonald, K., Wilson, R. F. (1997). Myocardial perfusion reserve: assessment with multisection, quantitative, first-pass MR imaging. *Radiology* 204:373–384.

Williams, D. S., Grandis, D. J., Zhang, W., Koretsky, A. P. (1993). Magnetic resonance imaging of perfusion in the isolated rat heart using spin inversion of arterial water. *Magn. Reson. Med.* 30:361–365.

Wilson, R. F., Marcus, M. L., White, C. W. (1987). Prediction of the physiological significance of coronary arterial lesions by quantitative lesion geometry in patients with limited coronary artery disease. *Circulation* 75(4):723–732.

Ye, F. Q., Mattay, V. S., Jezzard, P., Frank, J. A., Weinberger, D. R., McLaughlin, A. C. (1997). Correction for vascular artifacts in cerebral blood flow values measured by using arterial spin tagging techniques. *Magn. Reson. Med.* 37:226–235.

# Request Permission or Order Reprints Instantly!

## Request Permission/Order Reprints

Reprints of this article can also be ordered at
http://www.dekker.com/servlet/product/DOI/101081JCMR120030571